

# **Minimization of the surface roughness of gold films for Casimir force measurements**

Amy Proctor

University of Florida  
Chan Lab

August 1, 2006

## ABSTRACT

The Casimir force is a quantum electromagnetic effect that generates a force between two neutral, conducting plates held parallel in a vacuum. This force is only influential on the sub-micron scale, so any surface roughness of the components will directly affect the measured magnitude of the force. In this study, silicon substrates and glass spheres were cleaned and coated via sputter deposition with 35Å Ti and 2000 Å Au in preparation for Casimir force measurements. The samples' surface roughness was analyzed at every stage in their fabrication via atomic force microscopy. Plasma cleaning was applied both *in situ* and *ex situ*, and sputtering parameters such as power and magnetron sources were varied. The best parameters for gold sputter deposition were found to be 3mtorr pressure, 100W power, and use of an RF magnetron rather than a DC magnetron. Under these conditions, gold-coated silicon wafers with peak-to-peak variations of ~10nm and gold-coated glass spheres with variations of ~30-40nm were fabricated for use in future experimental Casimir force measurements.

## INTRODUCTION

As micromechanical devices become smaller and smaller, the force resulting from the Casimir effect becomes increasingly visible. Although negligible in the macroscopic world, the Casimir force can have very clear effects in the realms of micro- and nanotechnology [1-3]. Therefore, studying and measuring the Casimir force is vital for continuing the trend toward smaller yet functional devices. In order to pursue this research, however, the issue of surface roughness must be addressed. Excessive surface roughness impedes Casimir force experimentation and limits its applications [4-6].

The Casimir force was first predicted by Hendrik Casimir in 1948 while he was working with colloidal solutions and studying the van der Waals forces [7]. This initial discovery in the context of molecules was then extended to the typical scenario for the Casimir force, which requires that two neutral conducting plates in a vacuum be held parallel to one another, preferably at submicron distances, while the force between them is measured.

The Casimir force arises due to zero-point fluctuations in the quantum electromagnetic field. For each frequency  $w$ , the zero-point energy equals the value for half the energy of a photon [7]. When they are being reflected back and forth in a cavity, the frequencies can theoretically cause either an attractive force, if they do not correspond to the cavity resonance, or a repulsive force, if the vacuum field is amplified inside the cavity [7].

Generally, these scenarios both contribute; however, the resulting force is typically slightly more attractive than repulsive due to a greater pressure outside the cavity than within it because of excluded wavelengths. The accepted relationship dictates that the Casimir force is directly

proportional to the cross-sectional area of the plates and inversely proportional to the fourth power of the distance between the plates [8]. This means that as the distance between the plates decreases, the Casimir force rapidly becomes more influential. Because of its importance when working with very small scales, the Casimir force can directly affect the way that microelectromechanical systems (MEMS) operate. It can either become a part of the MEMS' functionality, by causing mechanical motion, or a hindrance to its correct operation, through stiction and other similar problems [1-3].

To measure the Casimir force experimentally, a sphere coated with a metal film is often used in conjunction with one metal plate instead of the historical arrangement requiring two conducting plates. This experimental layout results from the difficulty in keeping two plates perfectly parallel at submicron separations [1]. Although using a sphere eliminates that challenge, it augments another common obstruction toward measuring the Casimir force, which is the aforementioned issue of surface roughness. Creating a conducting plate with minimal roughness is far less complicated than creating a sphere with a smooth metal film. Most methods of depositing metal generate particles, which make Casimir force measurements at small separations challenging. Additionally, even measurements taken at larger separations are affected by the inconsistent distances between the experimental components [4-6].

In order for the Casimir force to be predictable and useful in MEMS or any other small devices, surface roughness must be analyzed and controlled. This is particularly important in the case of the spheres, because even commercially available glass spheres (100 microns in radius) have a variation in surface height exceeding 20 nm. However, the roughness after the deposition of metal is the more significant problem. Since the

Casimir effect is directly related to the separation between the surfaces of the sphere and the plate, special attention has to be paid to the way in which the metal film is deposited. Sputtering is often the deposition process chosen. Although it results in relatively smooth films over a short distance, sputtering can generate scattered clumped particles that are devastating to Casimir force measurements.

For this reason, sputtering parameters such as RF vs. DC power and chamber pressure were varied, and the resulting spheres and wafers were analyzed via atomic force microscopy (AFM) for effects on surface morphology. We also considered the effectiveness of oxygen and argon plasma cleaning. Analyses were performed at every increment in the process in order to isolate the advantageous factors.

Ultimately, if surface roughness can be reduced, better measurements of the Casimir force can be taken at submicron distances. This progress should facilitate the trend toward smaller devices without disruption from undesired quantum effects.

#### PRIMARY EQUIPMENT ANNOTATION: AFM and Sputtering

Atomic force microscopy (AFM) relies on a type of scanning probe microscope with a cantilever, a very sharp tip, a laser, and a photodiode as can be seen in Figure 1. We used a NT-MDT Solver PRO Scanning Probe Microscope in TappingMode™ or semi-contact mode. This means that the cantilever is not in full contact with the sample but rather resonates near the sample, touching it only at a certain point during its oscillation [9-10]. Because of the contact with the surface of the sample, the cantilever's amplitude varies. Piezoelectric ceramics provide extremely precise positioning of the sample or the tip. A laser reflected off the cantilever onto a photodiode gives feedback

about the cantilever's motion and about the distance change necessary to keep the oscillation amplitude constant. The laser's feedback is interpreted by the accompanying computer software, Nova Solver, in order to generate a topographical image.

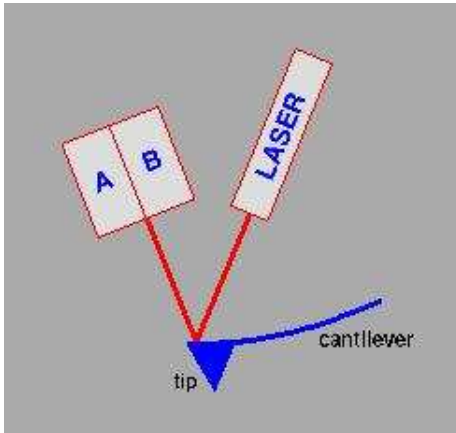


Figure 1. AFM Layout  
(<http://spm.phy.bris.ac.uk/techniques/afm/>)

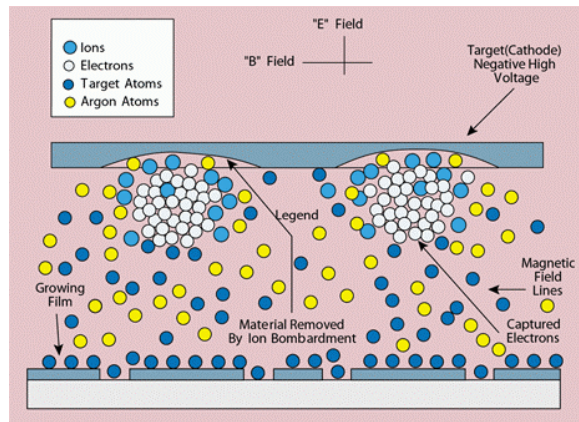


Figure 2. Diagram illustrating the process of metal sputtering  
(<http://www.vacgen.com/catalogue/section-16/intro.htm>)

Metal deposition by sputtering, at its most basic level, is the displacement of atoms on the surface of a sample by sputtered target atoms. An inert gas, usually argon, is ionized to generate plasma that bombards the target material, propelling target atoms toward the sample to be coated [11-12]. As can be seen in Figure 2, electrons and ions in the chamber initiate the propulsion of the target atoms, which are then accelerated by the electric field so that they slightly erode the sample surface as they collect there. We used the Kurt J. Lesker CMS-18 Multi-Target Sputter Deposition system, which has two vacuum chambers and four magnetron targets. Our system is capable of RF or DC fields. RF sputtering is typically reserved for insulators because it avoids excessive charge build-up at the magnetron but reduces the deposition rate. Sometimes, though, the slowed rate of RF sputtering is beneficial even when using metallic targets because the diminution of active atoms can lead to less clumping [13].

## INITIAL SPHERE ANALYSIS

First, in order to start with the smoothest possible spheres, we analyzed the surface morphology of spheres composed of a variety of materials, such as PMMA, glass, and polystyrene. We used AFM for obtaining information about the variations in surface height on the spheres. The PMMA and glass spheres (100 microns in radius) were the two smoothest, with peak to peak variations generally less than 30nm. Tables I and II detail the results. For the remainder of the experiment, we used only PMMA and glass spheres. AFM images of these two types of spheres are also included as Figures 3-6.

The following data were obtained from roughness analyses performed by Nova Solver using the feedback from the microscope. The microscope's input was first used to create images, such as the subsequent figures, and then those images were analyzed by the software for quantitative surface inconsistencies. The identified scan sizes refer to the linear dimensions of the images, and the grayscales vary by image as implied by the corresponding peak-to-peak variations.

sphere number	scan size (microns)	peak-to-peak variation (nm)	root-mean-sq. variation (nm)
1	5	21	1.7
1	1	7.0	0.50
2	5	18	1.6
2	1	6.7	0.61
3	10	28	1.7
3	5	17	1.5
4	10	26	2.0
4	1	4.8	0.45

TABLE I. AFM data for glass spheres

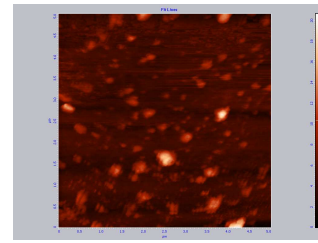


Fig. 3. 5-micron scan of glass sphere

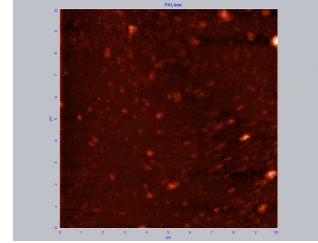


Fig. 4. 10-micron scan of glass sphere

sphere number	scan size (microns)	peak-to-peak variation (nm)	RMS variation (nm)
1	5	25	2.3
1	1	13	1.3
2	5	23	2.1
2	1	11	1.1
3	5	22	1.7
4	5	52	3.0
5	10	55	3.5
5	5	31	2.9

TABLE II. AFM data for PMMA spheres

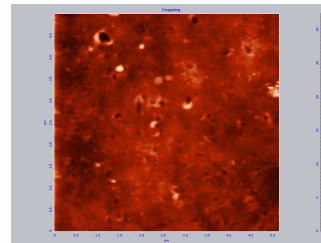


Fig. 5. 5-micron scan of PMMA

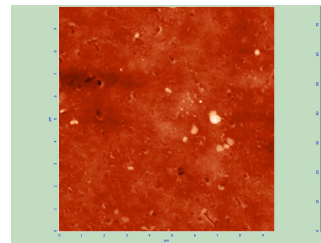


Fig. 6. 10-micron scan PMMA

## SUBSTRATE PREPARATION

Silicon wafers coated in Shipley 1813 Photoresist (PR) were cleaved and cleaned in acetone for five minutes. This process ensured that any particles generated by the cleaving did not remain on the silicon surface. After soaking the wafers in acetone to remove the PR, we moved them to isopropyl alcohol and immediately airbrushed them with nitrogen gas. Using isopropyl alcohol gave us more time to dry the wafers before the solution evaporated and therefore helped keep contamination from lodging onto the surface. The final cleaning step was a 20-minute oxygen plasma clean that was run in the Anatech SCE600 Asher with 600W power. Table III and Figure 7 show that this cleaning process resulted in surfaces with 2-12nm height variations.

area number	scan size (microns)	peak-to-peak variation (nm)	RMS variation (nm)
1	10	12	0.44
1	5	7.8	0.45
2	10	7.9	0.35
2	1	2.1	0.23
3	10	10	0.42

TABLE III. AFM data for clean Si wafers

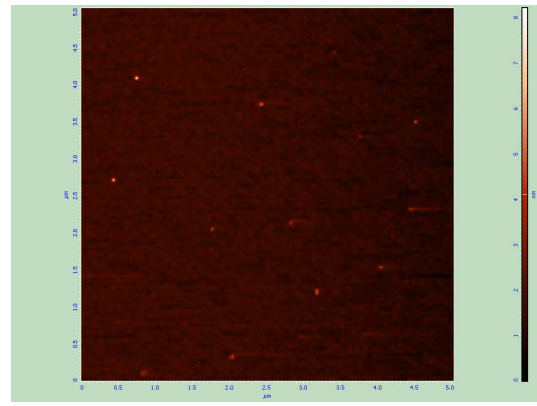


Fig. 7. 5-micron scan of cleaned Si

#### METAL DEPOSITION- DC Magnetron

After we determined the type of spheres to use and prepared the wafers, we began coating them with gold. Gold, however, does not adhere particularly well to our materials, so we used a 35 Å seed layer of titanium. This was applied from a DC magnetron at 250W and 5mtorr at a deposition rate of approximately 1 Å /sec. Then, we coated the spheres under standard conditions for gold (i.e., DC target at 150W and pressure at 5mtorr) to a thickness of approximately 2000 angstroms according to the accepted deposition rate of 5 Å /sec under these conditions. However, these parameters were insufficient for generating the necessary smoothness, as can be seen in Tables IV and V and Figures 8-11.

The first parameter adjustment made to the sputtering process was a reduction in the DC magnetron power from 150W to 90W. This caused little if any improvement in the final surface roughness, so data are comparable to those presented in Tables IV and V and Figures 8-11.

sphere number	scan size (microns)	peak-to-peak variation (nm)	RMS variation (nm)
1	5	61	4.8
1	1	22	2.0
2	5	84	6.0
2	1	26	3.2
3	3	34	3.7
3	10	99	6.7

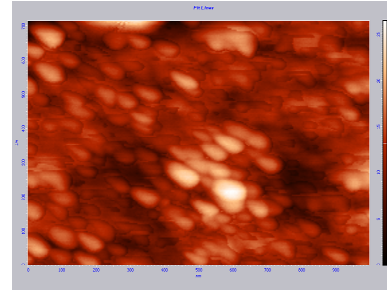


Fig. 8. 1-micron scan of glass + Ti + Au

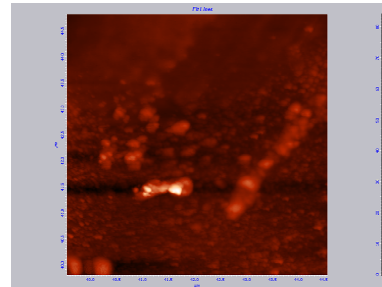


Fig. 9. 5-micron scan of glass + Ti + Au

TABLE IV. AFM data for glass + 35Å Ti + 2000Å Au (DC magnetron)

sample area	scan size (microns)	peak-to-peak variation (nm)	RMS variation (nm)
1	10	20.	1.3
1	1	9.0	1.2
2	10	22	1.3
2	5	14	1.3
3	10	32	1.4
3	10	23	1.2

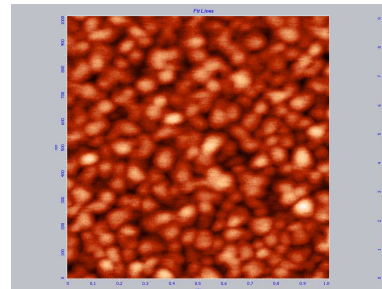


Fig. 10. 1-micron scan of Si + Ti + Au

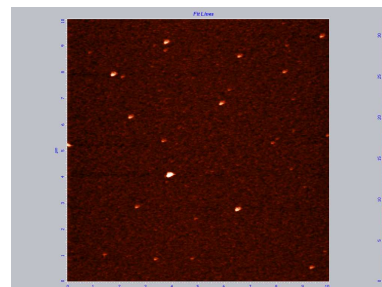


Fig. 11. 10-micron scan of Si + Ti + Au

TABLE V. AFM data for Si + 35Å Ti + 2000Å Au (DC magnetron)

METAL DEPOSITION- RF Magnetron

We chose to switch to a radio frequency (RF) magnetron despite its slower deposition rate because of the potential for less clumping. We also reduced the pressure from 5mtorr to 3mtorr. The deposition rate for gold at these parameters was unknown, so a metal liftoff was used to determine this rate. We prepared the silicon substrate as described previously, then coated it in PR via the Laurell Spinner WS-400A 6NPP/Lite at 5000 rpm to a thickness of 1.367 microns. Next, we exposed the PR for 17 seconds with the Karl Suss MA-6 Contact Mask Aligner using a mask that created 3-micron trenches. The PR was developed in M-319 developer for 45 seconds, and then the sample was rinsed with DI water and dried with nitrogen gas.

Subsequently, the wafer was coated with gold in the sputtering machine by the RF magnetron at 3mtorr and 100W for 950 seconds. We then dissolved the PR and determined that the film thickness was approximately 1000A by use of the Tencor Alphastep 200 Profilometer. The Profilometer operates by scanning the sample surface with a diamond-tipped stylus and then generating a graph of the surface height variations along the scanned line.

The glass and PMMA spheres coated by a RF magnetron at 3mtorr pressure and 100W power had average peak to peak variations of only 50nm. Additionally, the silicon wafers coated at these settings showed drastic improvement, from a peak to peak variation of approximately 20nm to one of only 10nm. Complete data can be found in Tables VI and VII and Figures 12-15.

sphere number	scan size (microns)	peak-to-peak variation (nm)	RMS variation (nm)
1	10	50.	3.9
1	5	51	3.3
2	5	42	5.3
2	5	74	7.4
3	5	62	5.1
3	5	46	4.9

TABLE VI. AFM data for glass spheres coated with 35A Ti and 2000A Au (RF magnetron)

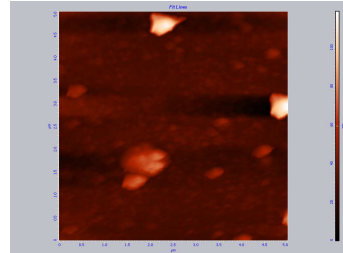


Fig. 12. 5-micron scan, glass + Au (RF)

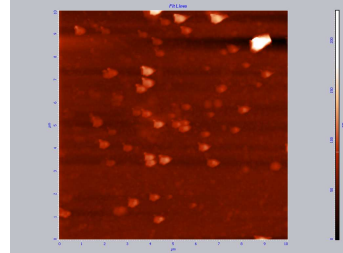


Fig. 13. 10-micron scan, glass + Au (RF)

sample area	scan size (microns)	peak-to-peak variation (nm)	RMS variation (nm)
1	10	8.4	0.86
1	5	6.6	0.48
2	10	10.	0.65
2	5	7.1	0.61
3	10	14	1.8
3	10	12	1.9

TABLE VII. AFM data for Si wafers coated with 35A Ti and 2000A Au (RF magnetron)

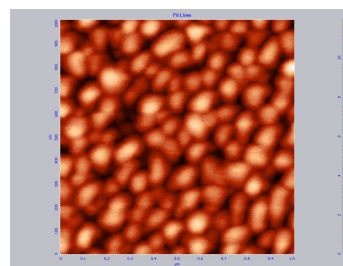


Fig. 14. 1-micron scan, Si + Au (RF)

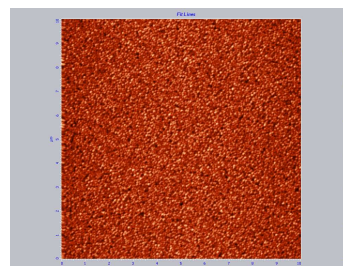


Fig. 15. 10-micron scan Si + Au (RF)

After this improvement in sputtering parameters, the silicon samples were acceptably smooth but pre-treatments for the spheres had to be added to the procedure to further minimize surface inconsistencies. We performed a 20-second oxygen plasma clean followed by a 5-second argon plasma clean done *in situ* immediately before depositing the metals. The oxygen plasma helped clean the surface by reacting with any organic

contamination, and the argon plasma physically bombarded the surface to free any remaining particles [14]. This cleaning method proved too harsh for the PMMA spheres; however, for the glass spheres, the times were adequately short to be beneficial without damaging the surface during the collision-based argon cleaning. We confirmed these findings with further AFM analysis.

Finally, with this preparation complete, we coated the glass spheres with 35A Ti and 2000A Au under the aforementioned optimized sputtering conditions. These spheres were then analyzed via AFM. These final data can be found in Table VIII, and two of the AFM images are included as Figures 16 and 17.

sphere number	scan size (microns)	peak-to-peak variation (nm)	RMS variation (nm)
1	5	23	2.7
1	10	36	2.4
2	10	46	4.9
2	5	36	4.5
3	5	30	2.9
3	10	35	2.8

TABLE VIII. AFM data for glass spheres plasma cleaned and coated with 35A Ti and 2000A Au (RF magnetron)

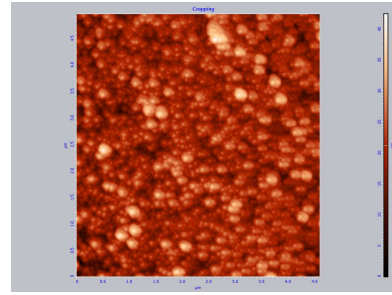


Fig. 16. 5-micron scan of glass + Ti + Au

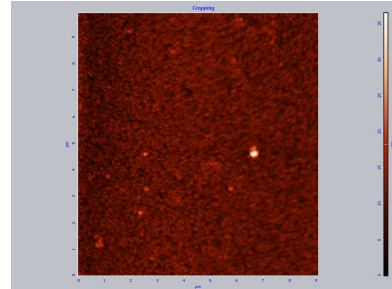


Fig. 17. 10-micron scan of glass + Ti + Au

## DISCUSSION

The final AFM images and data of the glass spheres and silicon substrates coated in gold demonstrate the amount of improvement made by adding pre-treatments like plasma

cleaning and changing the sputtering parameters. The resulting samples have far fewer irregularities in general, and those that remain are significantly smaller. After changing parameters in increments and checking for roughness at every point, we can confidently report that the improvements in the surface morphology are the direct result of the plasma cleaning processes and the optimized sputtering parameters, specifically the use of an RF magnetron.

Despite these improvements, more can always be accomplished in this field. Another aspect that could be considered is the deposition means itself. We only varied parameters within the context of sputtering deposition, but other deposition methods could be considered as well, along with their individual conditions. Regardless of the deposition means used, further analysis could be performed on resulting samples in order to determine aspects like surface potential. More studies must be carried out to explore other possible routes and to guarantee that these results are applicable to other materials.

Although research of this genre is never truly finished, overall, the roughness of the samples was approximately halved by the progress made during this study. This result should be beneficial to experimental measurements of the Casimir force because it will allow for smaller separations between the sphere and plate being used and will result in more accurate measurements. Additionally, these parameters for sputtered-gold deposition can be applied to other research in which gold-film roughness is a concern.

## ACKNOWLEDGMENTS

I would like to thank Dr. H.B. Chan for advising me on this project, Dr. I. Kravchenko and B. Lewis for their assistance with the equipment operation and advice about which

parameters to alter, and Yiliang Bao, graduate student, for her assistance with every aspect of the project. I would also like to thank the University of Florida Physics Department for hosting this REU and the NSF for funding this program.

## REFERENCES

- [1] H.B. Chan, V.A. Aksyuk, R.N. Kleiman, D.J. Bishop, and F. Capasso, *Science* **291**, 1941 (2001).
- [2] E. Buks and M.L. Roukes, *Phys. Rev. B* **63**, 033402 (2001).
- [3] S.K. Lamoreaux, *Phys. Rev. Lett.* **78**, 5 (1997); **81**, 5475(E) (1998).
- [4] G. Palasantzas, *J. Appl. Phys.* **97**, 126104 (2005).
- [5] T. Ederth, *Phys. Rev. Lett.* **62**, 062104 (2000).
- [6] S.K. Lamoreaux, *Phys. Rev. Lett.* **83**, 16 (1999).
- [7] A. Lambrecht, *Phys. World* **15**, 9 (2002).
- [8] H.B.G. Casimir, *Proc. K. Ned. Akad. Wet.* **51**, 793 (1948).
- [9] G. Binnig, C.F. Quate, and Ch. Gerber, *Phys. Rev. Lett.* **56**, 9 (1986).
- [10] Q. Zhong, D. Inniss, K. Kjoller, and V.B. Elings, *Surf. Sci.* **290**, 10 (1993).
- [11] P. Sigmund, *Phys. Rev.* **184**, 2 (1969).
- [12] S. A. Bashar, “Study of ITO for Novel Optoelectronic Devices,” thesis, Univ. of London (1998).
- [13] D. Barreca, A. Gasparotto, E. Tondello, G. Bruno, and M. Losurdo, *Appl. Phys.* **96**, 3 (2004).
- [14] T.C. Isabell, P.E. Fischione, C. O’Keefe, M.U. Guruz, and V.P. Dravid, *Microsc. Microanal.* **5**, 126-135 (1999).